Received: 28 February 2018 | Accepted: 15 April 2018

DOI: 10.1002/jbio.201800067

Journal of BIOPHOTONICS

FULL ARTICLE

In vivo study of rat cortical hemodynamics using a stereotaxic-apparatus-compatible photoacoustic microscope

Heng Guo[1,2] | Qian Chen[1,2] | Weizhi Qi[1,2] | Xingxing Chen[2] | Lei Xi[1,2]*

[1]Department of Biomedical Engineering, Southern University of Science and Technology, Shenzhen, China

[2]School of Physics, University of Electronic Science and Technology of China, Chengdu, China

***Correspondence**
Lei Xi, Department of Biomedical Engineering, Southern University of Science and Technology, Shenzhen, Guangdong 518055, China.
Email: xilei@sustc.edu.cn

Funding information
Department of Science and Technology of Sichuan Province, Grant/Award Number: 2016HH0019; National Natural Science Foundation of China, Grant/Award Numbers: 61775028, 81571722, 61528401; Southern University of Science and Technology

Brain imaging is an important technique in cognitive neuroscience. In this article, we designed a stereotaxic-apparatus-compatible photoacoustic microscope for the studies of rat cortical hemodynamics. Compared with existing optical resolution photoacoustic microscopy (ORPAM) systems, the probe owns feature of fast, light and miniature. In this microscope, we integrated a miniaturized ultrasound transducer with a center frequency of 10 MHz to detect photoacoustic signals and a 2-dimensional (2D) microelectromechanical system (MEMS) scanner to achieve raster scanning of the optical focus. Based on phantom evaluation, this imaging probe has a high lateral resolution of 3.8 μm and an effective imaging domain of 2×2 mm^2. Different from conventional ORPAMs, combining with standard stereotaxic apparatus enables broad studies of rodent brains without any motion artifact. To show its capability, we successfully captured red blood cell flow in the capillary, monitored the vascular changes during bleeding and blood infusion and visualized cortical hemodynamics induced by middle cerebral artery occlusion.

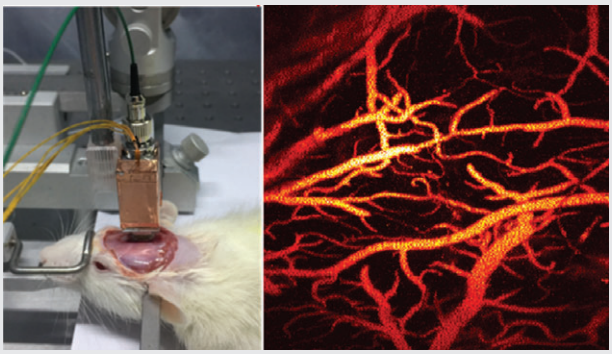

KEYWORDS
brain imaging, cortical hemodynamics, photoacoustic microscope

1 | INTRODUCTION

As the most important research and clinical tool in neuroscience, brain imaging allows to directly observe both mental processes and cognitive activities in vivo [1]. Most ongoing brain studies focus on applying imaging technologies to explore the structure, function and metabolism of brain activities [2]. In clinic, x-ray computed tomography (XCT), magnetic resonance imaging (MRI) and positron emission tomography (PET) are irreplaceable to screen brain diseases via abnormal structural, functional and metabolic changes in human brain [3–5]. XCT scan has advantages of cost-efficiency, high-speed, high-resolution and deep penetration. However, besides incapability of deriving functional parameters, it still suffers from ionizing radiation. MRI is one of the most powerful imaging tools to study brain structures. In addition, functional MRI (fMRI) has successfully demonstrated to investigate various brain disorders and cognitive activities in clinic. Unfortunately, high cost and low temporal resolution make it accessible to limited research and clinical institutes. PET, providing both functional and metabolic information of brain, is able to capture early-stage and metastatic brain tumors. However, the spatial resolution is low and potential ionizing radiation is nonignorable.

With the rapid development of laser techniques, optical imaging modalities such as confocal microscopy,

epifluorescence microscopy, 2/multiphoton microscopy and optical coherence tomography angiography (OCTA) have been extensively applied to study brain disorders and cognitive activities in fundamental research [6–9]. Benefiting from miniaturization of optical components, it is feasible to carry out studies in awake and freely moving rodents using optical imaging techniques [10]. For epifluorescence and 2/multiphoton microscopy, it is easy to visualize neurons and blood vessels with the use of external contrast agents. However, it is challenging to accurately derive vascular functional parameters such as oxy/deoxy-hemoglobin concentrations, oxygen consuming rate and oxygen saturation using exogenous contrast agents. OCTA is sensitive to blood flow and capable of imaging cortical vasculatures in high resolution. Besides, visible light-based OCTA has been demonstrated for deriving the oxygenation [11].

Photoacoustic imaging, a hybrid imaging modality, features rich optical contrast, high acoustic resolution, multiscale imaging capability and ultrahigh sensitivity to hemoglobin [12, 13]. It has been successfully demonstrated in both clinical and fundamental studies including early-stage cancer diagnosis, arthritis detection, drug/nanomaterial evaluation and brain research [14–18]. Photoacoustic microscopy, especially optical resolution photoacoustic microscopy (ORPAM), has been extensively applied in studying cortical hemodynamic in animals due to the excellent sensitivity to endogenous hemoglobin inside blood vessels, comparable penetration depth with 2/multiphoton microscopy, and identical resolving capability with pure optical microscopies [19, 20]. The use of new scanner and fast laser sources promotes the development of compact and miniaturized ORPAMs, which are suitable for brain imaging and reveal the potential to carry out studies in awaking animals [21–23]. Unfortunately, none of them is compatible with stereotaxic apparatuses, which are widely used in brain operations from animals to humans due to the bulky size and innegligible weight. In this report, we report a stereotaxic-apparatus-compatible high-resolution photoacoustic microscope by using a 2-dimensional (2D) microelectromechanical system (MEMS) scanner, which is light, fast and owns a large scanning optical angle. Combined with stereotaxic apparatus, we carry out in vivo studies of rat cortical hemodynamics including observation of the cell flow in a single capillary, monitoring the vascular changes during the procedures of blood extraction and infusion, as well as visualizing cortical hemodynamics induced by middle cerebral artery occlusion (MCAO).

2 | METHODS

2.1 | System configurations

Figure 1A shows the schematic of the stereotaxic-apparatus-compatible photoacoustic microscope. We used a high-repetition-rate (up to 50 kHz) laser with a duration of 5 nanoseconds (ns). Light pulses are focused into a 15-μm pinhole for spatial filtering, and then coupled into a single mode fiber by a space-to-fiber coupler (APFC-5T-FC, Beijing Zolix Instruments Co., Beijing, China). Figure 1B illustrates the layout of the photoacoustic imaging probe. The output laser pulses from the fiber is collimated by a fiber collimator (F220FC-532, Thorlabs Inc., Shanghai, China), converged by a doublet lens (GCL-010601, Daheng Optics, Beijing, China), and re-directed to the MEMS scanner using a right angle prism (MRAP1-4.0, MT Optics, Fuzhou, China). The MEMS scanner (WM-L5-5, WiO Tech, Wuxi, China) is driven by a multifunctional data acquisition card (PCI-6731, National Instrument, Texas) to realize fast raster scanning of the focused laser beam. An ultrathin cover glass is tilted with an angle of 45° in a small water cube to reflect the photoacoustic signals and allow the transmission of the light beam. An unfocused ultrasonic transducer with a center frequency of 10 MHz, a bandwidth of 80% and an active aperture of 2 mm is used to detect the photoacoustic signals. The PA signals are amplified by an amplifier (5073-PR, Olympus Inc., Beijing, China) at ~39 dB and digitized with a high-speed data acquisition card (ATS-9325, Alazar Inc., Canada). Figure 1C shows photographs of the imaging probe, which weights 20 g and is fixed on a manipulator of the stereotaxic apparatus. During the experiments, the imaging probe is adjusted to image the selected area of the rat brain (Figure 1A). The gap between the brain and the imaging probe is filled with saline, which serves as the coupling medium for ultrasound transmission and maintains the conservation of osmotic pressure inside and outside the brain.

2.2 | Phantom preparation

To evaluate the spatial resolution of the system, a sharp blade was positioned horizontally on the surface of a tissue-mimicking phantom. The background of the phantom was made by the mixture of agar, deionized water, India ink and intralipid to simulate the optical properties of the biological tissue, which has an optical absorption coefficient of 0.007 mm^{-1} and a reduced optical scattering coefficient of 1.0 mm^{-1}.

2.3 | Animal handling

For regular brain imaging, 5 female Wistar rats (250-300 g) were anesthetized with chloral hydrate (50 mg/kg) by intraperitoneal injection and maintain the body temperature at 37°C using a heating pad. We fixed the heads of the rats using the stereotaxic apparatus and did craniotomies over the right parietal bone. The dura was kept intact and continually bathed with artificial cerebrospinal fluid. We adjusted the probe and carried out full-view imaging of a 2 × 2 mm^2 region in the brain using a frame size of 500 × 500, and small domain imaging in a region of 50 × 50 μm^2 using a frame size of 80 × 80. Considering that the laser emits

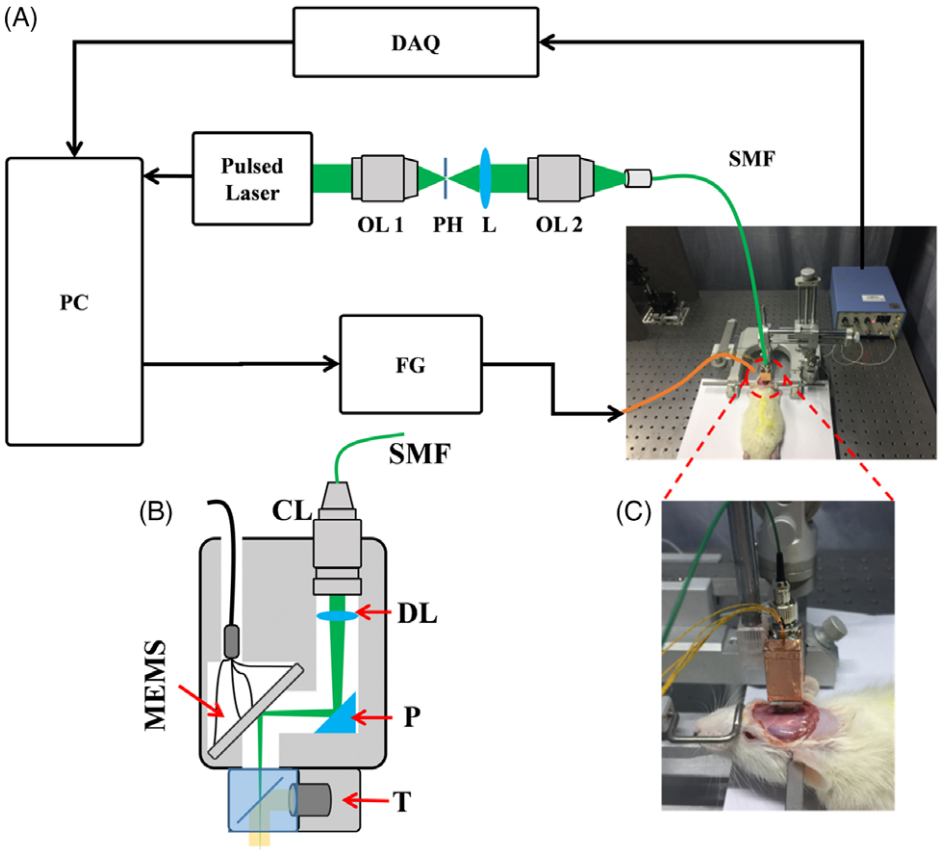

FIGURE 1 Schematic of the photoacoustic imaging system and probe. (A) The configuration of the imaging system and the photograph of the stereotaxic-integrated imaging interface. (B) The detail schematic of the imaging probe. The green beam depicts the illumination light path, the blue presents the deionized water and the yellow part indicates the acoustic detection path. (C) Photograph of the rat receiving imaging. OL, objective lens; PH, pinhole; L, lens; SMF, signal mode fiber; DAQ, data acquisition card; FG, function generator; CL, collimator lens; DL, doublet lens; P, prism; T, transducer

50 000 pulses/s, it takes 5 seconds for a full-view image and 0.128 seconds for small domain imaging.

To show the cortical hemodynamics induced by bleeding and blood infusion, a total number of 5 female Wistar rats, weighting from 250 to 300 g, were anesthetized and maintained by supplements of one-sixth of the initial dose at an interval of ~30 minutes during the experiments. Two PE-50 cannulas were inserted into the femoral arteries on both sides to measure the blood pressure and extract blood to induce brain hemodynamics. Another cannula was inserted into the femoral vein to infuse heparin sodium solution and blood. We measured the blood pressure using a pressure transducer and a multiparameter physiological monitor (RM6240, Chengdu Instrument Inc., Chengdu, China). We carried out 10 full-view experiments as the resting state with a time interval of 1 minute before the extraction of blood, then extracted the blood with a constant velocity until blood pressure dropped to 40 mmHg, in which we captured additional 10 images. Blood pressure was maintained at 40 mmHg and we continually monitored the same imaging region for additional 25 minutes. The infusion was conducted with injection of the blood via femoral vein and additional 10 images were captured. We carried out additional 25 experiments every 1 minute to monitor the vascular changes postinfusion.

We established the MCAO model using another 5 female Wistar rats. Transient MCAO was induced surgically in the rat brains following the method reported by Uluc et al. [24]. A Y-shaped artery consisted of the external, internal and common carotid artery (ECA, ICA and CCA) was dissected first. Then, the ECA was tied off using a suture, and another suture was placed loosely around the bifurcation of the Y-shaped artery. After the CCA and the ICA were clipped near the bifurcation using vessel clips, an incision in the ECA was created between 2 sutures. A nylon suture with a silicon-coated tip was inserted from the ECA to the ICA. Finally, the incision from the neck was closed.

All the animal studies have been approved by the ethic committee at the Southern University of Science and Technology (SUSTech). After the experiments, all mice were sacrificed using SUSTech-approved standard procedures.

3 | RESULTS AND DISCUSSIONS

Figure 2A,B shows the photoacoustic maximum amplitude projection (MAP) image and the corresponding Gaussian-fitted profile of the imaged blade edge indicated by the red dashed line, respectively. We derives the line spread function (LSF) and calculating the full width at half maximum (FWHM) of the LSF, which is 3.8 μm and represents the experimental lateral resolution of the system [21–23]. The theoretical lateral resolution, which depends on the numerical aperture of doublet lens, is 3.2 μm. This discrepancy is mainly caused by the unflatten MEMS scanner surface and mismatch of reflective indexes among air, glass and water in the light path. As shown in Figure 2C, the FWHM of the Gaussian-fitted axial profile of a typical depth-resolved PA signal is ~104 μm, which agrees well with the theoretical

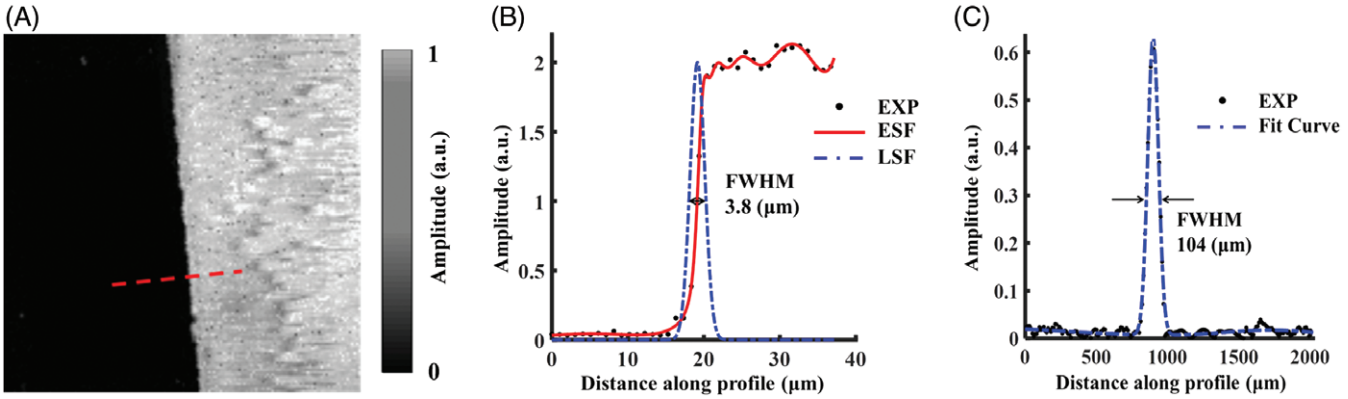

FIGURE 2 Evaluation of the system performance. (A) Photoacoustic MAP image of a surgical blade edge. (B) FWHM of the Gaussian-fitted lateral profiles of the blade edge. (C) FWHM of the Gaussian-fitted axial profile of a typical PA signal. EXP, experimental data; ESF, edge spread function

axial resolution (105 μm) calculated using the given center frequency and bandwidth of the transducer [21–23, 25].

To illustrate the structural imaging capability of the microscope to observe fast events, we imaged a rat brain with removal of the scalp and skull, in which multiscale blood vessels in the ultra-dense vascular network were clearly identified (Figure 3A). Figure 3B shows the enlarged MAP images of a single capillary in the cropped region by a white dashed rectangle in Figure 3A with a smaller frame size of 80 × 80 and a faster frame rate of 7.8125 Hz. Movie S1 presents the longitudinal monitoring of the capillary, in which we clearly observe the flow of the red blood cells. Four typical MAP slices are selected from the movie to display the distribution of cells in different time points (Figure 3B). Brain is the most important organ in various organisms, in which multiscale blood vessels serve as the nutrition deliver and are tightly associated with activations of neurons as well as numerous brain diseases. Red blood cells conjugated with hemoglobin are perfect photoacoustic absorbers and supply sufficient image contrast. Several high-speed ORPAMs show the encouraging studies of neurovascular coupling in anesthetized and restricted animal [20]. However, the inconvenience of the systems limits the studies to certain areas in the brain. Our probe is small and light enough to mount on the

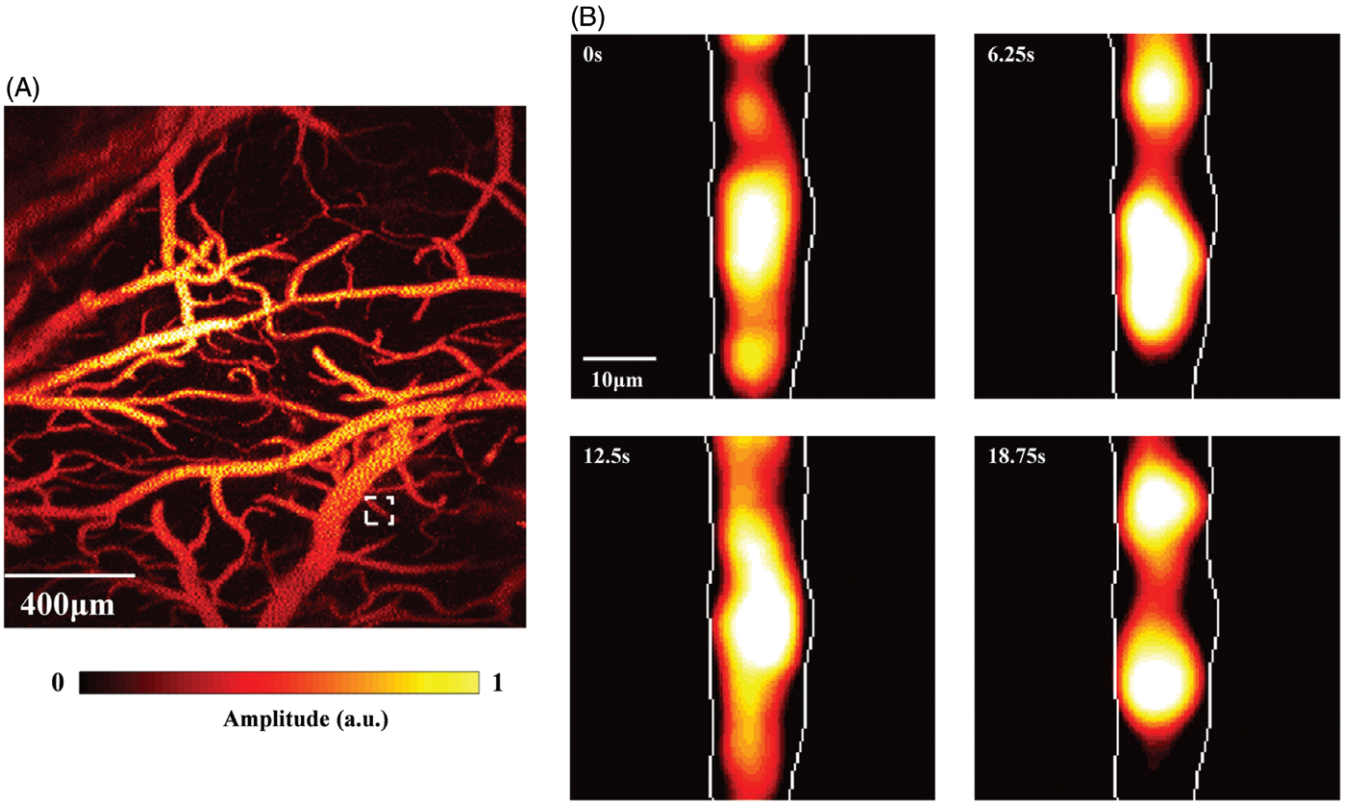

FIGURE 3 (A) in vivo imaging of the brain vasculature. (B) in vivo imaging of a single capillary indicated by white dashed line in (A). Movie S1 presents the flow of red blood cells in the capillary. Four typical slices selected from Movie S1 show the distribution of red blood cells in 4 different time points. The images have a frame size of 80 × 80, an FOV of 50 μm and a volume rate of 7.8125 Hz

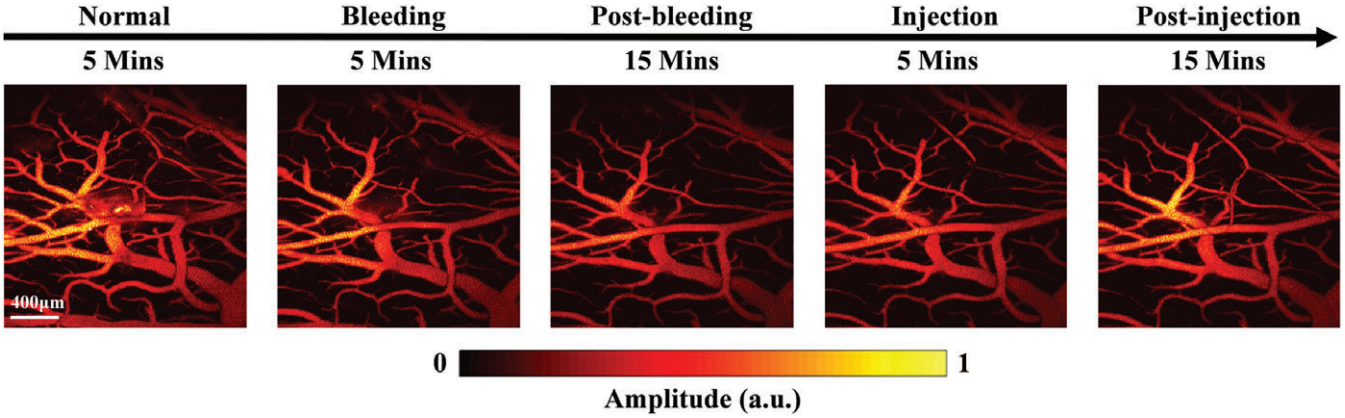

FIGURE 4 Five representative vascular images of a rat brain in different stages during bleeding and infusion including normal status, bleeding, postbleeding, rapid infusion and postinfusion

stereotaxic-apparatus, making it accessible to perform brain studies in any position. In addition, the probe owns features of high imaging quality and fast imaging speed, which allow to observe multiscale structures and fast events.

We established a rat model revealing hemodynamics in cerebral cortex of the brain, in which relatively complex surgeries prevented the movement of the animal during the imaging experiments, to show the advantages of the system in compactness and easy-to-use. Figure 4A shows 5 representative MAP images and Movie S2 displays vascular kinetics in a rat brain over the entire course of bleeding and infusion. There are 5 stages including normal status (10 minutes), bleeding (10 minutes), postbleeding (25 minutes), rapid infusion (10 minutes) and postinfusion (25 minutes). In the

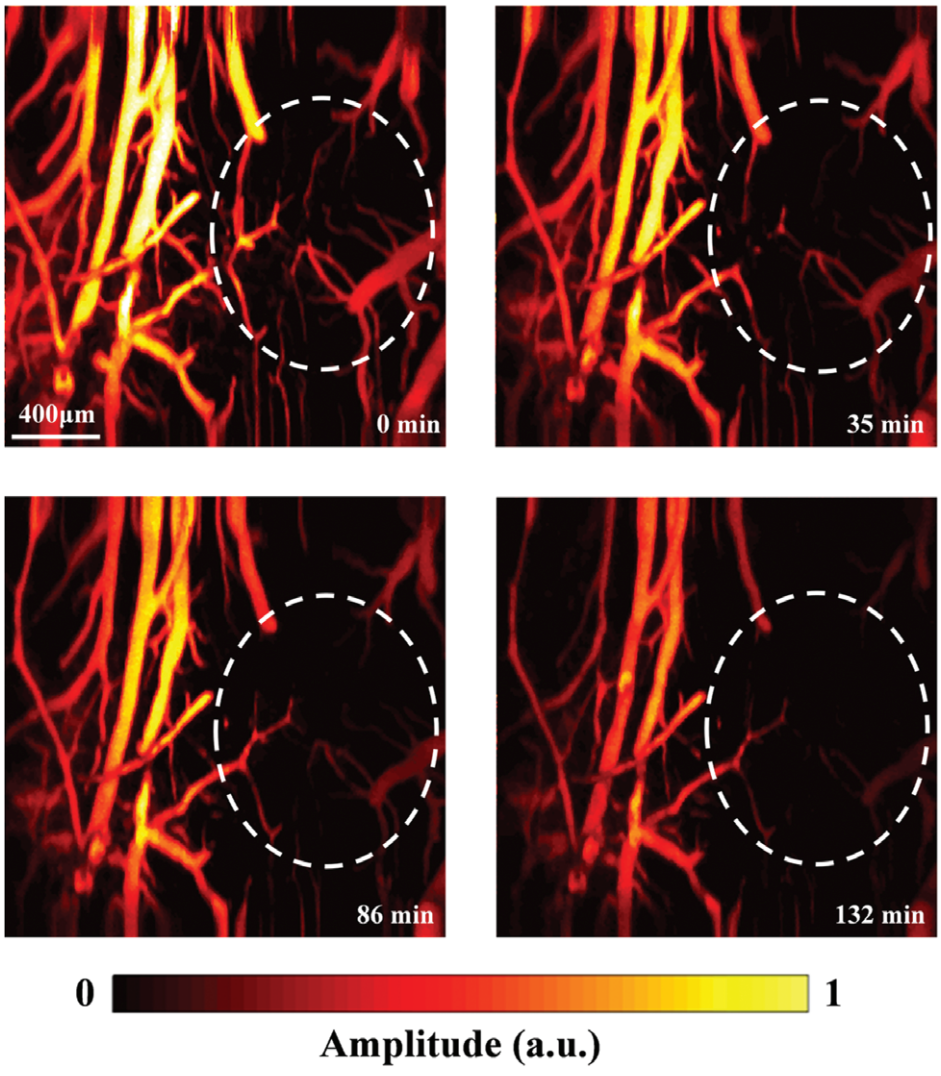

FIGURE 5 Four representative vascular images of a rat brain in different time points after the establishment of MCAO

normal status, there are numerous capillaries distributed in the brain. During the stage of bleeding via extraction of blood from the femoral artery, the PA amplitudes of both large blood vessels and capillaries start to decrease. The vessels start to shrink in order to compensate the loss of blood pressure. Then, the blood in the capillaries is dispatched to major blood vessels in the stage of postbleeding, leading to a low signal to noise ratio of capillaries. In the stage of rapid infusion with the injection of blood, both capillaries and large blood vessels start to recover.

In addition, we also observed the rat cortical hemodynamics induced by MCAO. Each experiment takes 132 minutes. Figure 5 presents 4 representative MAP images. At the beginning, we observe many capillaries in the brain. In about 30 minutes after the surgery, small blood vessels and capillaries in the region indicated by the dashed white circle start to disappear. Meanwhile, the big and medium vessels begin to shrink and the concentration of total hemoglobin (HbT) decreases significantly due to the insufficient supply of blood induced by MCAO. Movie S3 depicts the hemodynamic changes of the imaged area before and after the establishment of MCAO.

4 | CONCLUSION

In summary, we propose a stereotaxic-apparatus-compatible photoacoustic microscope, which can be used to observe the rat cortical hemodynamics in vivo. Combined with stereotaxic apparatus, this new microscope is able to get clear and stable vasculature in any regions over the entire rat cortical area. The use of a doublet lens and a 10 MHz acoustic transducer provides a high lateral resolution of 3.8 μm and a moderate axial resolution of 104 μm. We demonstrate that this system works well for different brain applications, and could become an ideal device for future brain studies. However, there are some limitations and several improvements needed to overcome and implement. First, a high-frequency ultrasound transducer and a high NA focusing lens can significantly improve the sensitivity and spatial resolution of the imaging system. Second, in terms of the temporal resolution, it is feasible to accelerate the imaging speed by using a faster scanner and laser source.

ACKNOWLEDGMENTS

This work was sponsored by National Natural Science Foundation of China (61775028, 81571722 and 61528401), Startup grant from Southern University of Science and Technology, State International Collaboration Program from Sichuan province (2016HH0019).

AUTHOR BIOGRAPHIES

Please see Supporting Information online.

REFERENCES

[1] N. Pouratian, S. A. Sheth, N. A. Martin, A. W. Toga, *Trends Neurosci.* **2003**, *26*, 277.
[2] A. H. Hielscher, *Curr. Opin. Biotechnol.* **2005**, *16*, 79.
[3] S. Arun, J. Ajith, P. M. R A, N. Raviteja, A. K. Muhammed, J. P G, M. Jayaprakash, N. Suresh, *Clin. Nucl. Med.* **2017**, *42*(1), e41.
[4] D. S. Kim, T. Q. Duong, S. G. Kim, *Nat. Neurosci.* **2000**, *3*, 164.
[5] C. J. Buckley, P. F. Sherwin, A. P. L. Smith, J. Wolber, S. M. Weick, D. J. Brooks, *Nucl. Med. Commun.* **2017**, *38*(3), 234.
[6] T. Kakimoto, *Histochem. Cell Biol.* **2017**, *7449*, 1.
[7] G. Kim, N. Nagarajan, E. Pastuzyn, K. Jenks, M. Capecchi, J. Shepherd, R. Menon, *Sci. Rep.* **2017**, *7*, 44791.
[8] S. Sakadzic, E. Roussakis, M. A. Yaseen, E. T. Mandeville, V. J. Srinivasan, K. Arai, S. Ruvinskaya, A. Devor, E. H. Lo, S. A. Vinogradov, D. A. Boas, *Nat. Methods* **2010**, *7*, 755.
[9] U. Baran, R. K. Wang, *Neurophotonics* **2016**, *3*, 010902.
[10] R. Cao, J. Li, B. Ning, N. Sun, T. Wang, Z. Zuo, S. Hu, *Neuroimage* **2017**, *150*, 77.
[11] S. Chen, Q. Liu, S. Tong, H. Zhang, presented at Optics and the brain **2017**, BrW3B.5.
[12] L. V. Wang, S. Hu, *Science* **2012**, *335*(6075), 1458.
[13] P. C. Beard, *Interface Focus* **2011**, *1*(4), 602.
[14] T. T. W. Wong, R. Zhang, P. Hai, C. Zhang, M. A. Pleitez, R. L. Aft, D. V. Novack, L. V. Wang, *Sci. Adv.* **2017**, *3*(5), e1602168.
[15] L. Xi, H. Jiang, *Appl. Phys. Lett.* **2015**, *15*(26), 18076.
[16] L. Xi, H. Jiang, *J. Biophotonics* **2016**, *9*(3), 213.
[17] J. F. Lovell, C. S. Jin, E. Huynh, H. Jin, C. Kim, J. L. Rubinstein, W. C. Chan, W. Cao, L. V. Wang, G. Zheng, *Nat. Mater.* **2011**, *10*(4), 324.
[18] J. Yao, L. Wang, J. M. Yang, K. I. Maslov, T. T. W. Wong, L. Li, C. Huang, J. Zou, L. V. Wang, *Nat. Methods* **2015**, *12*(5), 407.
[19] L. Lin, J. Yao, R. Zhang, C. Chen, C. Huang, Y. Li, L. Wang, W. Chapman, J. Zou, L. V. Wang, *J. Biophotonics* **2016**, *10*, 6.
[20] L. Xi, T. Jin, J. Zhou, P. Carney, H. Jiang, *Neuroimage* **2017**, *161*, 232.
[21] T. Jin, H. Guo, L. Yao, H. Xie, H. Jiang, L. Xi, *J. Biophotonics* **2018**, *11*, e201700250.
[22] T. Jin, H. Guo, H. Jiang, B. Ke, L. Xi, *Opt. Lett.* **2017**, *42*, 21.
[23] W. Qi, T. Jin, J. Rong, H. Jiang, L. Xi, *J. Biophotonics* **2017**, *10*(12), 1580.
[24] K. Uluç, A. Miranpuri, G. C. Kujoth, E. Aktüre, M. K. Başkaya, *J. Vis. Exp.* **2011**, *48*, e1978.
[25] S. P. Mattison, R. L. Shelton, R. T. Maxson, B. E. Applegate, *Biomed. Opt. Express* **2013**, *4*, 1451.

SUPPORTING INFORMATION

Additional supporting information may be found online in the Supporting Information section at the end of the article.

Movie S1. The longitudinal monitoring of the capillary.

Movie S2. Vascular kinetics in a rat brain during the entire course of bleeding and infusion.

Movie S3. The hemodynamic changes of the rat brain before and after the establishment of MCAO.

How to cite this article: Guo H, Chen Q, Qi W, Chen X, Xi L. In vivo study of rat cortical hemodynamics using a stereotaxic-apparatus-compatible photoacoustic microscope. *J. Biophotonics*. 2018; e201800067. https://doi.org/10.1002/jbio.201800067